ELSEVIER

Journal of Photochemistry and Photobiology A: Chemistry 113 (1998) 163–169

Journal of Photochemistry and Photobiology A:Chemistry

Photoinduced energy and electron transfers in the porphyrin triad (zinc octaethylporphyrin-4,4′ bipyridinium-tetraphenylporphyrin)$^{2+}$, 2 ClO4^{-})

Mohamed El Baraka [a,*], Jean Marc Janot [a], Laurent Ruhlmann [b], Alain Giraudeau [b], Michel Deumié [c], Patrick Seta [a]

[a] *Laboratoire des Matériaux et Procédés Membranaires, CNRS UMR 5635, 1919 Route de Mende, 34293 Montpellier Cedex 05, France*
[b] *Laboratoire d'Electrochimie et de Chimie Physique du Corps Solide, CNRS URA 405, Université Louis Pasteur, 67008 Strasbourg, France*
[c] *Laboratoire de Chimie physique, Université de Perpignan, 52 Avenue de Villeneuve, 66860 Perpignan Cedex, France*

Received 1 October 1997; accepted 15 November 1997

Abstract

Intramolecular electron and energy transfers were investigated in a series of porphyrin molecules linked to a bipyridinium cation, by steady state absorption and emission spectroscopies, time resolved fluorescence and voltammetry. A strong quenching of the fluorescence intensity related to an important intramolecular electron transfer was observed when bipyridinium moiety V was attached either to the zinc (A) or to the free base porphyrin (B) in dyads AV and BV. This intramolecular electron transfer operates from the photoexcited singlet state of the zinc porphyrin (^{1}A) or of the free-base porphyrin (^{1}B) to the bipyridinium mono or dication moiety resulting in charge separation and formation of biradical state A·$^+$V· or B·$^+$V·. The electron transfer rate constants of this process in AV$^+$ and BV$^+$ were 3.8×10^9 s^{-1} and 7.7×10^9 s^{-1}, respectively. In the case of heteroporphyrin triad AV^{2+}B where metallo and free-base porphyrins were attached to the bipyridinium spacer, both energy transfer and electron transfer processes were observed. The quantum yield of the singlet–singlet energy transfer which explains most of the quenching was 0.77 and the corresponding rate constant was 4.9×10^9 s^{-1}. In addition, both first excited states ^{1}AV^{2+}B and AV^{2+} ^{1}B decayed via photoinduced electron transfers to produce radical ion pairs A·$^+$V·$^+$B and AV·$^+$B·$^+$. An energy levels diagram of the various S_1 states of triad AVB is proposed and the efficiency of the various transfer processes also discussed.

Keywords: Absorption; Fluorescence; Porphyrin; Lifetime; Electron transfer; Energy transfer

1. Introduction

Energy transfer and electron transfer between aromatic molecules have been extensively studied over the past few years. These studies have been extended to metalloporphyrins, because these molecules represent an ideal model to understand the photosynthesis phenomenon in the bacteria and green plants. The conversion of excitation energy into chemical potential in photosynthetic reaction centers involves a photoinduced electron transfer from the chlorophyll excited singlet state which generates charge separated species.

The increasing interest in the photophysical and photochemical characteristics of the porphyrins prompts more and more workers to synthesize porphyrin and metalloporphyrin derivatives: on one hand 'face to face' molecules in which two porphyrins (donor–acceptor) are held in parallel conformation and separated by various distances [1–9], and on the other hand, donor–acceptor covalently linked molecules which mainly consist of a porphyrin as a donor and quinones, viologens or other small organic molecules as acceptors [10–24]. These research works are focused on the kinetic studies of the charge separation and charge recombination processes which depend on the redox potentials, the distance between the acceptor and the donor, and the nature of the linkage between them.

Electron transfer and electronic energy transfer have been demonstrated in a variety of cases [3,4,7,13,16] depending on the intramolecular distance between the chromophores and their relative orientations. According to some authors [7,8] the zinc porphyrin molecules must be in close proximity and well oriented with respect to the copper porphyrin molecules so that energy transfer can easily take place. A number of

* Corresponding author.

1010-6030/98/$19.00
PII S1010-6030(97)00329-8

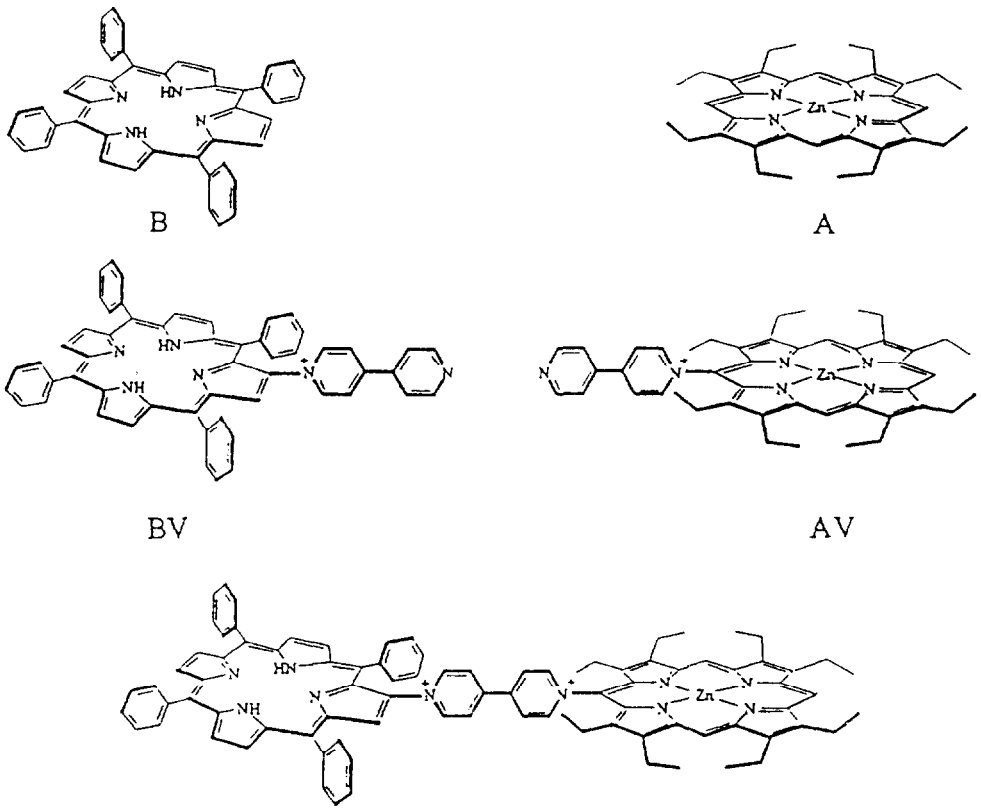

Fig. 1. Structures of bipyridinium-linked porphyrins.

groups have found that the electronic structure of the spacer plays an important role in the electron transfer rate; they have shown that for a 4 Å donor–acceptor distance the transfer rate is more decreased with an aliphatic spacer than with an aromatic one [4,8,10].

In the present work, we have investigated the nature and the relative efficiencies of the electron transfer and energy transfer processes in metallo and free-base porphyrins attached to a bipyridinium acceptor (dyads) and in the bis-porphyrin (triad) compound where the two porphyrins are rigidly connected by a bipyridinium (viologen) spacer as shown in Fig. 1.

2. Experimental

2.1. Materials

Zinc octaethylporphyrin A and 4,4′ bipyridine were purchased from Aldrich, tetraphenylporphyrin (free base) B was prepared and purified by known procedures [25,26]. The preparation of complexes AV^+, BV^+ and $AV^{2+}B$ has been previously reported [27].

The solvent C_2H_5OH was reagent grade quality, used without further purification. The supporting electrolyte, tetrabutylammonium perchlorate (Fluka), was recrystallized from 60:40 (v/v) ethanol/water and dried under vacuum at 70°C for 48 h. All solvents used for the spectroscopic measurements were spectrograde from Sigma or Aldrich.

2.2. Measurements

All electrochemical measurements were carried out under argon. Voltammetric data were obtained with a standard three electrode system using a Bruker E 130 M potentiostat and a high-impedance millivoltmeter (minisis 5000, Tacussel). Current-potential curves were obtained from an Ifelec If 3802 X–Y recorder. The working electrode was a platinum disk (E.D.I. type, Solea Tacussel) of 3.14 mm^2 surface area. A platinum wire was used as the auxiliary electrode. The reference electrode was a saturated calomel electrode (SCE) that was connected to the studied solution by a junction bridge filled with the supporting electrolyte solution.

The absorption spectra were recorded on a UV visible Kontron 940 spectrophotometer. Corrected fluorescence spectra were taken on a SPF-4800 (SLM Aminco) spectrofluorimeter with slit widths of 4 nm for both excitation and emission spectra.

The fluorescence lifetimes were measured by using the time correlated single photon counting technique. The excitation pulse was fed by a spectra Physics mode locked argon laser, model 2030, and by a synchronously pumped Spectra

Physics (rhodamine 6G) dye laser, model 375. The repetition rate of the dye laser was 82 MHz, the duration pulse about 10 ps and the average power 100 mW. The time between two successive excitation pulses was controlled by means of a cavity dumper Spectra Physics model 344, the frequency being reduced to 4 MHz. The fluorescence collected at 90° of the excitation was detected by a multichannel plate photomultiplier Hamamatsu model 1564 after passage through a JOBIN YVON monochromator model H10 for the selection of the desired emission wavelength and a Glan–Taylor prism (emission polariser) set to the magic angle (54.73°). The response function of the apparatus (time amplitude converter ORTEC model 457, multichannel analyser TRACOR NORHERN model 1750) was in the 100 ps range (FWHM), measured by scattering the excitation light in a dilute solution of ludox. The pump profile was accumulated using the same count rate and the same number of counts at the maximum of the decay curve (about 3×10^4 counts) or 2×10^6 counts for the integrated decay. The decay curve was fitted by convolution of the fluorescence decay calculated as $I(t) = \sum a_i \cdot \exp(-t/\tau_i)$, where a_i and τ_i are the amplitude and lifetime of the different components of the total fluorescence emission $I(t)$ at time, t, respectively, with the excitation profile obtained from the scattering sample. The fitting procedure (using the Marquardt algorithm) was achieved when the value of the statistical χ^2 criterion reached a minimum. A histogram of detected photons was collected on a the multichannel analyser and subsequently transferred to a Hewlett-Packard (HP 9000) computer for analysis.

3. Results

3.1. Electrochemistry

The electrochemical behaviour of the porphyrins A and B is well documented [28–30]. In the potential range of −2 V to +2 V the electron transfer on the ring occurred via two reversible one electron reductions and two reversible one electron oxidations. In the presence of the electroactive group bpy^+ or bpy^{2+} (V^{2+} moiety) the electrochemical reduction and oxidation of A and B occurred on both sides of the electroactivity range of these groups. The electrochemical results are gathered in Table 1.

The electrochemical behavior of AV^+, BV^+ and $AV^{2+}B$ in $CH_3CN/1,2\text{-}C_2H_4Cl_2$ (1:4 v/v) has been previously presented [25]. We examined their redox behavior in C_2H_5OH which presented a limited electroactivity range compared to $CH_3CN/1,2\text{-}C_2H_4Cl_2$. In this solvent, no changes were detected in the electrochemical comportment of the studied complexes. As expected, the presence of an electron withdrawing group shifted the oxidation potentials towards more positive values. The recorded voltammogram of triad $AV^{2+}B$ appeared as the superposition of the voltammogram of the corresponding subunits AV^+ and BV^+. The main effect of the substitution concerned the mechanism of the oxidation of free base porphyrin B. Complex BV^+ was oxidized at +1.25 V/SCE via an irreversible two-electron transfer in contrast with the two distinct monoelectronic oxidation steps of free base B.

In triad $AV^{2+}B$, the oxidation of B occurred at the same potential as the oxidation of A (second step). In consequence, an oxidation wave at +1.29 V/SCE in C_2H_5OH which corresponds to an exchange of three electrons was observed. This implies that abstraction of only one electron of the free base in triad $AV^{2+}B$ is not obvious. This situation might be related to the complex fluorescence spectrum observed with $AV^{2+}B$.

3.2. Absorption spectra

The absorption spectra of the five porphyrins studied exhibit a Soret band near 400 nm and several Q-bands in the 500 to 700 nm range. The absorption maxima of the studied compounds are listed in Table 2. The absorption spectrum of triad $AV^{2+}B$ is essentially a linear combination of the absorption spectra of dyads AV^+ and BV^+, with only minor differences in wavelength maxima and band shapes. In Fig. 2 are presented the absorption spectra of AV^+, BV^+ and $AV^{2+}B$ and the linear combination of the spectra of dyads

Table 1
Electrochemical data for the studied porphyrins and bisporphyrins

Compounds	Porphyrin ring oxidation		bpy^+ or $bpy2^+$ reduction		Porphyrin ring reduction		
	$E_{1/2}^{II}$	$E_{1/2}^{I}$	$E_{1/2}^{II}$	$E_{1/2}^{I}$	$E_{1/2}^{I}$	$E_{1/2}^{II}$	$E_{1/2}^{III}$
H_2TPP	1.31	1.07			−1.18	−1.48	[a]
ZnOEP	1.06	0.68.			−1.60		[a]
$H_2TPP\text{-}\beta\text{-}Bpy^+$		$1.25^{irr,2e}$	−0.73		−1.12	−1.40	[a]
(BV)		$1.25^{irr,2e}$	−0.73		−0.81	−0.95	[b]
$ZnOEP\text{-}bpy^+$	$1.20^{irr,e}$	0.91	−0.65		−1.31		[a]
(AV)	$1.18^{irr,e}$	0.93	−0.71		−0.85		[b]
$H2TPP\text{-}\beta\text{-}bpy\text{-}ZnOEP^{2+}$	$1.22^{irr,3e}$	0.93	−0.59	−0.06	−1.18	−1.41	−1.61 [a]
(BVA)	$1.29^{irr,3e}$	0.98	−0.49	−0.04	$-1.21^{irr,e}$		[b]

All potentials in V/SCE were obtained from (RDE) voltammetry in: [a] $CH_3CN/1,2\text{-}C_2H_4Cl_2$ (1:4), tetraethylammonium perchlorate 0.1 M (see Ref. [25]); [b] C_2H_5OH, tetrabutylammonium perchlorate 0.1 M. The working electrode was Pt. All steps were reversible one-electron transfer except those with superscript.

Table 2
Absorption maxima (nm) of A, B, AV^-, BV^+, and $AV^{2+}B$ in ethanol

Compounds	Soret bands	Q bands			
A	406	–	537	574	–
AV^+	414	–	543	580	–
B	414	511	547	591	646
BV^+	419	521	–	599	654
$AV^{2+}B$	421	–	544	580	649

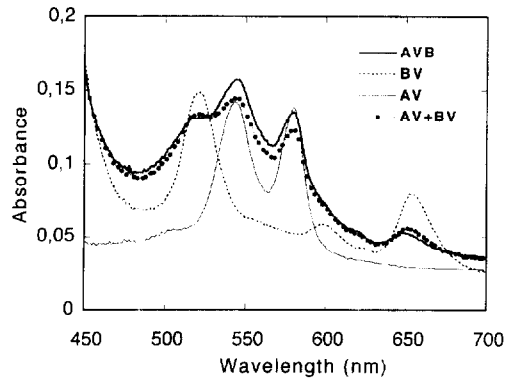

Fig. 2. Absorption spectra of ethanol solutions of dyads AV^+ and BV^+, and triad $AV^{2+}B$ and linear combination ($\cdots\bullet\cdots$) of the spectra of AV^- and BV^+ which approximate that of heterotriad $AV^{2+}B$.

AV^+ and BV^+ implied in the description of heterotriad $AV^{2+}B$. Consistent with the absorption spectra obtained, only weak interactions between the different moieties occur in the S_0 state. As expected, these composite molecules retain the individual identities of the starting chromophores.

3.3. Fluorescence spectra

For all five studied molecules the fluorescence spectra were taken in the same conditions and a common excitation wavelength at 411 nm was selected. Besides, all solutions were adjusted to the appropriate concentrations able to give the same absorbance at that wavelength. The fluorescence spectrum of A presented two maxima at 580 nm and 625 nm; free-base porphyrin B presented maxima at 650 nm and 720 nm (Table 3).

As expected from the general behaviour of donor/acceptor entities in which the bipyridinium acceptor is non fluorescent, a fluorescence quenching was observed when passing from the individual species A or B to dyads AV^+ or BV^+. Comparative studies were performed for these porphyrins in dichloromethane (dielectric constant $\varepsilon = 9.08$) and ethanol ($\varepsilon = 24.3$). They demonstrated that no large solvent effect related to noticeable changes in charge separation occurred in these molecules. The fluorescence intensity was strongly quenched in the case of model compounds AV^+ and BV^+ as compared to the fluorescence intensity observed in the case of A and B (Fig. 3) while the fluorescence shape was not modified. This is explained by the presence of the covalently linked bipyridinium acceptor. On the basis of considerable

Table 3
Maxima of the fluorescence spectra of A, B, AV^+, BV^+, and $AV^{2+}B$ in ethanol

Compounds	$\lambda_{fluo,\,Max}$				
A	580	625			
$A-V^+$	581	623			
B			650		720
$B-V^+$			650	670	720
$AV^{2+}B$	580	625	650	690	

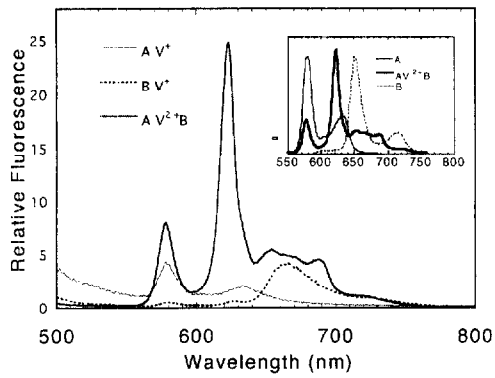

Fig. 3. Steady-state fluorescence emission spectra of triad $AV^{2+}B$, dyads AV^+ and BV^+, and in the insert of zinc porphyrin A and free-base porphyrin B. All spectra were recorded at 293 K in ethanol at the fixed excitation wavelength of 411 nm and corrected.

previous works [16,31] this result is ascribed to rapid exothermic electron transfer from the excited porphyrin to the bipyridinium acceptor. In EtOH we find for free-base compound BV^+ a relative quantum yield $\phi/\phi_0 = 0.023$, ϕ_0 being the fluorescence quantum yield of the corresponding free-base monomer B. Likewise, for zinc dyad AV^+ we obtain $\phi/\phi_0 = 0.016$, ϕ_0 being in the latter case the fluorescence quantum yield of zinc porphyrin monomer A.

On the contrary, the shape of the fluorescence spectrum of triad $AV^{2+}B$ appears very complex as compared to the fluorescence spectra of monomers A and B. The $AV^{2+}B$ fluorescence cannot be obtained by any combination of the two separate emissions of A and B (see Fig. 3). This reveals that some important interactions must be established between the different moieties in the excited state.

3.4. Excitation spectra

The excitation spectra of $AV^{2+}B$ determined in EtOH solution was corrected for the wavelength dependence of the efficiency of the excitation source. The emission was monitored at 720 nm where the fluorescence comes from free-base porphyrin B. We have verified that individual excitation spectra of both AV^+ and BV^+ contribute to the excitation spectrum of $AV^{2+}B$ (not shown). It is clear that absorption of light by both porphyrin moieties contributes strongly to the emission. For instance, the $AV^{2+}B$ excitation spectrum (Table 2) contains the 521 nm absorption band of the BV^+

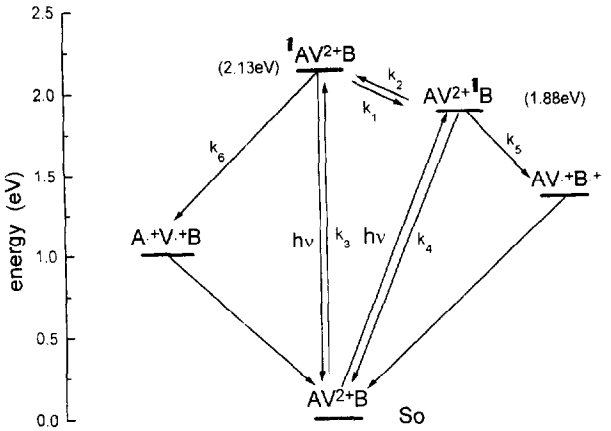

Fig. 4. Energies of the first excited porphyrin singlet state and charge-separated states of heterotriad $AV^{2+}B$, based on results for the component monomers and associated interconversion pathways.

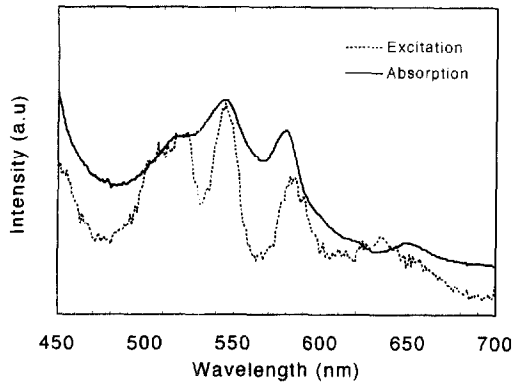

Fig. 5. Absorption spectrum and corrected fluorescence excitation spectrum of triad $AV^{2+}B$ (λ_{em} = 719 nm), 10^{-5} M in ethanol. The excitation spectrum was monitored at the fluorescence wavelength of 719 nm where only free-base porphyrin moiety B emits significantly. Both spectra were normalized at 510 nm.

moiety (511 nm absorption band for free base porphyrin B) along with the 543 and 580 nm bands of AV^+ (537 and 574 nm for zinc porphyrin A). In triad $AV^{2+}B$ the zinc porphyrin moiety A acts as a donor by transferring some singlet excitation energy to the attached free-base B (step 1 in the general energy diagram drawn in Fig. 4). However, the corrected excitation spectrum does not coincide with the absorption spectrum (Fig. 5). The fact that the spectra are not identical in the region where the zinc porphyrin moiety absorbs strongly indicates that singlet–singlet energy transfer is incomplete. Since all the emission at 720 nm comes from free base porphyrin B, the singlet energy transfer efficiency was, as a first approximation, estimated by finding the fraction of the absorption spectrum of AV^+ which, when added to that of BV^+, best reproduces the shape of the corrected excitation spectrum shown in Fig. 5. The transfer coefficient calculated in this way was 0.77 ± 0.10.

3.5. Time-resolved fluorescence studies

The fluorescence quenchings noted in the steady state spectra of dyads AV^+ and BV^+ were similarly observed in time-resolved studies. Excitation of free base porphyrin B and zinc porphyrin A in EtOH solution at ambient temperatures with 587 nm laser pulses resulted in the observation of a single exponential decay (similar to that was already determined [31]) with lifetimes of 2 ns ($\chi^2 = 1.06$) and 9 ns ($\chi^2 = 1.06$) for A and B, respectively. Similar experiments with dyads AV^+ and BV^+ showed that the fluorescence decay profiles consist of a sum of two decays. The corresponding lifetimes were 0.265 and 1.8 ns ($\chi^2 = 1.22$) for AV^+, 0.127 and 7.8 ns ($\chi^2 = 1.12$) for BV^+. The components of the fluorescence decays with the shorter lifetimes of AV^+ and BV^+ may arise from the direct quenching of the photoexcited singlet state of the porphyrin by the bound bipyridinium. The longer lifetimes were close to those of A and B. Similar results have been obtained for viologen linked porphyrins [31]. The decay curves of the fluorescence spectrum at eleven different wavelengths were measured for triad $AV^{2+}B$ in EtOH under the same excitation conditions. These curves were best fitted by four exponential decay times ($\chi^2 = 1.23$) as shown in Fig. 6. The two major contributions to the decay-associated spectra had lifetimes of 0.157 and 1.9 ns (see Table 4). Although the global fluorescence spectrum of $AV^{2+}B$ is not any simple sum of A and B spectra, the 0.157 ns component presented the general emission shape of zinc porphyrin moiety A, and its high amplitude is consistent with the fact that the major

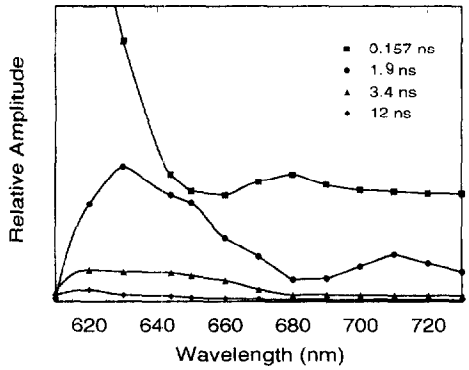

Fig. 6. Decay-associated spectra of triad $AV^{2+}B$ in ethanol obtained with 587 nm excitation. The fluorescence decays at the thirteen indicated wavelengths were analyzed globally to yield the characteristic lifetimes shown with a χ^2 value of 1.23. As indicated in the text, the major components present lifetimes of 0.157 ns and 1.9 ns. The minor component lifetimes are 3.4 ns and 12 ns.

Table 4
Lifetimes and intramolecular energy (k_f) and electron transfer (k_{et}) rate constants of A, B, AV^+, BV^+, and $AV^{2+}B$

Compounds	τ (ns)				χ^2	k_f (s^{-1})	k_{et} (s^{-1})
A		2			1.06		
A–V^+	0.265	1.8			1.22		3.8×10^9
B				9.0	1.12		
B–V^+	0.127			7.8	1.12		7.7×10^9
AV^{2+}–B	0.157	1.9	3.4	12	1.23	4.9×10^9	9.7×10^8; 4.2×10^8

part of the light at 587 nm is absorbed by that chromophore. It then follows that 0.157 ns is the lifetime of $^1AV^{2+}B$ in which only the ^1A moiety is analysed. The 1.9 ns component had the spectral features of both Zn porphyrin A at 630 nm and free base porphyrin B at 650 nm and 710 nm, the two other lifetimes (minor components), contributing to less than 5% (see Fig. 6) to the total decay amplitude at all wavelengths are presumably caused by the presence of impurities in the solution and will be ignored.

4. Discussion

The lowest singlet state energies of A and B calculated from the wave number average between absorption and emission of the reddest absorption maximum for each porphyrin were 2.13 and 1.88 eV, respectively. The energy diagram given in Fig. 4 shows the energy levels of the excited states of heterotriad $AV^{2+}B$. This diagram based on the various results experimentally obtained for all monomer components is constructed from the excited state energy levels of the individual entities and from the respective redox potentials of the donors A and B and of the acceptor V in the dyads and in the triad. Excited singlet states $^1AV^{2+}B$ and AV^{2+} ^1B differ in energy by 0.25 eV. This difference means that the singlet energy transfer from free base porphyrin B to zinc porphyrin A via step 2 (Fig. 4) should be very slow compared to step 1 because it is an endergonic process. We observed in the case of $^1AV^{2+}B$ a decrease (from 2 ns (^1A) to 0.157 ns ($^1AV^{2+}B$)) in the lifetime of the zinc porphyrin first excited state due to an energy transfer from A to B. The singlet–singlet energy transfer was further investigated using steady state fluorescence excitation spectroscopy. The corrected excitation spectrum was normalized to the value of the absorption spectrum of triad $AV^{2+}B$ measured at 510 nm where most of the absorption is due to free base porphyrin B. The excitation spectrum had the characteristic features of both A and B due to the partial energy transfer between A and B. Quantitatively, the singlet–singlet energy-transfer quantum yield Φ_{ET} was approximately 0.77. The rate constant for step 1 (k_1) can thus be calculated from the relation

$$k_1=\phi_{ET}/\tau \quad (1)$$

in which ϕ_{ET} is the singlet energy transfer quantum yield and τ is the lifetime of the first excited state of $^1AV^{2+}B$; the k_1 value calculated from Eq. (1) is $4.9\times10^9\ s^{-1}$. Alternatively, one might be tempted to deduce k_1 from the lifetimes of $^1AV^+$ and $^1AV^{2+}B$, 265 ps and 157 ps, respectively. But the shorter lifetime of $^1AV^{2+}B$ should be due to the contribution of k_1 only if the non-radiative decays of $^1AV^{2+}B$ and AV^{2+} ^1B are identical with that of $^1AV^+$, which is unlikely.

Treating the interconversion of the two excited states $^1AV^{2+}B$ and AV^{2+} ^1B as an equilibrium process we can write:

$$\Delta G_0^*=RT\ln K=-0.25\ \text{eV} \quad (2)$$

The calculated equilibrium constant $K=k_1/k_2$ for the energy transfer was 1.7×10^4 at 298 K; the corresponding value of k_2 is $2.9\times10^5\ s^{-1}$. These results verify our hypothesis of the existence of a slow singlet–singlet energy transfer (if any) from free-base B to zinc porphyrin A via step 2 as shown in Fig. 4.

There are two reasonable explanations for the observed quenching of the zinc porphyrin first excited state. The first one is related to an energy transfer (step 1) as the time resolved fluorescence studies presented reveal that this indeed does occur. The second explanation takes into account an additional electron transfer (step 6); this electron transfer from the zinc porphyrin first excited state yields biradical $A\cdot^+V\cdot^+B$ via an exergonic process characterized by $\Delta G=-1.1$ eV and therefore should be considered as well. This possibility is consistent with the less than unity value calculated for the energy transfer efficiency obtained from the steady state fluorescence excitation experiments. So, if we consider now the direct electron transfer (step 6) and because the repopulation of $^1AV^{2+}B$ via step 2 is negligible, the lifetime of the zinc porphyrin first excited state will be

$$1/\tau=k_1+k_3+k_6 \quad (3)$$

The τ value was given above and k_3 may be estimated as $5\times10^8\ s^{-1}$ from the 2 ns fluorescence lifetime of the monomer zinc porphyrin which cannot undergo energy or electron transfer. It follows therefore that Eq. (3) gives a value of $9.7\times10^8\ s^{-1}$ for the electron transfer rate constant k_6 and the quantum yield of electron transfer from $^1AV^{2+}B$ to $A\cdot^+V.^+B$ via step 6 calculated from $k_6/(k_1+k_3+k_6)$ is 0.15. The longer lived component of B fluorescence (1.9 ns in Fig. 6) has the spectrum of the free base porphyrin moiety and therefore represents the decay of AV^{2+} ^1B. Two of the possibilities of the decay of this excited state are the singlet–singlet energy transfer (step 2) as discussed above and the decay via the usual photophysical processes lumped together as step 4.

The above analysis has shown that the energy transfer route (step 2) may be ignored. In addition, the rate constant k_4 for step 4 can be estimated as $1.11\times10^8\ s^{-1}$ from the 9 ns singlet excited state lifetime measured for free-base monomer B. Besides, neither step 2 nor step 4 can explain the relatively short lifetime of AV^{2+} ^1B and another quenching process must occur. Fig. 4 suggests that another deactivation pathway is the electron transfer from the free base to the pyridinium yielding $AV\cdot^+B\cdot^+$ by step 5.

It is clear from the energy diagram of Fig. 4 that whereas the $AV^+\cdot B^+$ state lies at about 1.33 eV above the ground state, the free base porphyrin excited singlet state energy is 1.88 eV. Thus, the photoinduced electron transfer is exergonic by about 0.55 eV and expected to be slower than k_6, which corresponds to an exergonic process of about 0.8 eV. The electron transfer rate constant k_5 estimated from the quenching of the fluorescence lifetime can be calculated from Eq. (4)

$$k_5=1/\tau-1/\tau_0 \quad (4)$$

where τ is the 1.9 ns component of the fluorescence decay of the triad and τ_0 is the lifetime of the free-base monomer (see Table 3) which cannot undergo electron transfer. The electron transfer rate constant k_5 calculated by this way is $4.15 \times 10^8\ s^{-1}$, indeed lower than k_6.

No transient absorption spectra of radicals or of triplet states have been recorded in nanosecond pulse laser absorption spectroscopy of the dyads and triad. Thus the back electron transfer rate is presumably very fast. This also is the reason why in the mechanistic scheme of Fig. 4 the triplet states have been ignored.

5. Conclusion

The steady state and time-resolved fluorescence data for the porphyrin dyads discussed above clearly demonstrate that electron transfers occur between the donors (zinc or free base porphyrin) and the bipyridinium acceptor. This electron transfer is very efficient in both AV^+ and BV^+ dyads as already established in similar previous transient absorption results [31]. The electron transfer is responsible for the observed fluorescence quenching of these dyads, as a result of charge separation leading to biradical states $A\cdot^+V\cdot$ and $B\cdot^+V\cdot$. Both electron transfer and energy transfer were observed in heterotriad $AV^{2+}B$. The singlet–singlet energy transfer from zinc porphyrin excited state $^1AV^{2+}B$ to the free base porphyrin yielding excited state $AV^{2+}\ ^1B$ is incomplete because its quantum yield is less than unity (0.77), but it appears as the major quenching process. In addition, both first excited singlet states $^1AV^{2+}B$ and $AV^{2+}\ ^1B$ of the porphyrin triad decay via photoinduced electron transfer to produce radical ion pairs $A\cdot^+V\cdot^+B$ and $AV\cdot^+B\cdot^+$.

References

[1] A. Osuka, K. Maruyama, N. Mataga, T. Asahi, I. Yamazaki, N. Tamai, J. Am. Chem. Soc. 112 (1990) 4958–4959.
[2] A.M. Brun, A. Harriman, V. Heitz, J.P. Sauvage, J. Am. Chem. Soc. 131 (1991) 8657–8663.
[3] D. Heiler, G. McLendon, P. Rogalskyj, J. Am. Chem. Soc. 109 (1987) 604–606.
[4] A. Helms, D. Heiler, G. McLendon, J. Am. Chem. Soc. 113 (1991) 4325–4327.
[5] J.M. De Graziano, P.L. Lanna Leggett, A.L. Moore, T.A. Moore, D. Gust, J. Phys. Chem. 98 (1994) 1758–1761.
[6] A. Helms, D. Heiler, G. McLendon, J. Am. Chem. Soc. 114 (1992) 6227–6238.
[7] J.M. Lang, H.G. Drickamer, J. Phys. Chem. 97 (1993) 5058–5064.
[8] T. Nagata, Bull. Chem. Soc. Jpn. 64 (1991) 3005–3016.
[9] F. Scandola, R. Argazzi, C.A. Bignozzi, M.T. Indelli, J. Photochem. Photobiol., A: Chem. 82 (1994) 191–202.
[10] K. Hashroni, H. Levanon, J. Tang, M.K. Bowman, J.R. Norris, D. Gust, T.A. Moore, A.L. Moore, J. Am. Chem. Soc. 112 (1990) 6477–6481.
[11] P. Siddarth, R.A. Marcus, J. Phys. Chem. 96 (1992) 3213–3217.
[12] S. Nishitani, N. Kurata, Y. Sakata, S. Misumi, M. Migita, T. Okada, N. Mataga, Tetrahedron Lett. 22 (1981) 2099–2102.
[13] J. Kroon, H. Oevering, J.W. Verhoeven, A.M. Olivier, M.N. Paddon-Row, J. Phys. Chem. 97 (1993) 5065–5069.
[14] P.J.G. Coutiho, S.M.B. Costa, J. Photochem. Photobiol., A: Chem. 82 (1994) 149–160.
[15] D. Gust, T.A. Moore, P.A. Liddell, G.A. Nemeth, L.R. Makings, A.L. Moore, D. Barrett, P.J. Pessiki, R.V. Bensasson, M. Rougée, C. Chachaty, F.C. De Schryver, M. Van der Auweraer, A.R. Holzwarth, J.S. Connolly, J. Am. Chem. Soc. 109 (1987) 846–856.
[16] A.L. Rieger, J. Edwards, G. Levey, Photochem. Photobiol. 38 (1983) 123–129.
[17] L.R. Khundkar, J.W. Perry, J.E. Hanson, P.B. Dervan, J. Am. Chem. Soc. 116 (1994) 9700–9709.
[18] Z. Wang, W.G. McGimpsey, J. Phys. Chem. 97 (1993) 5054–5057.
[19] K. Kikuchi, T. Niwa, Y. Takahashi, H. Ikeda, T. Miyashi, J. Phys. Chem. 97 (1993) 5070–5073.
[20] P.J.G. Coutiho, S.M.B. Costa, Chem. Phys. 182 (1994) 399–408.
[21] J. Pouliquen, V. Wintgens, J. Chem. Phys. 85 (1988) 456–472.
[22] Y. Sakata, H. Tsue, M.P. O'Neil, G.P. Wiederrecht, M.R. Wasielewski, J. Am. Chem. Soc. 116 (1994) 6904–6909.
[23] J.L.Y. Kong, K.G. Spears, P.A. Loach, Photochem. Photobiol. 35 (1981) 545–553.
[24] A.D. Joran, B.A. Leland, G.G. Geller, J.J. Hopfied, P.B. Dervan, J. Am. Chem. Soc. 106 (1984) 6082–6091.
[25] A.D. Alder, F.R. Longo, J.D. Finareli, J. Goldmacher, J. Assour, L. Korskoff, J. Org. Chem. 32 (1967) 476.
[26] G.H. Barnett, M.F. Hudson, K.M. Smith, Tetrahedron Lett. 30 (1973) 2887–2888.
[27] A. Giraudeau, L. Ruhlmann, L. El Kahef, M. Gross, J. Am. Chem. Soc. 118 (1996) 2669–2979.
[28] J. Fajer, D.C. Borg, A. Forman, D. Dolphin, R.H. Felton, J. Am. Chem. Soc. 92 (1970) 3451–3459.
[29] J.H. Fuhrhop, D. Mauzerall, J. Am. Chem. Soc. 91 (1969) 4178–4181.
[30] A. Giraudeau, H.J. Callot, J. Jordan, J. Ezhar, M. Gross, J. Am. Chem. Soc. 101 (1979) 3857–3862.
[31] J. Hirota, I. Okura, J. Phys. Chem. 97 (1993) 6867–6870.